

Inviscid fluid flow in an accelerating cylindrical container

By R. E. MOORE AND L. M. PERKO

Lockheed Missiles and Space Company, Palo Alto, California

(Received 16 October 1964)

The problem of the axially symmetric irrotational flow of an inviscid incompressible fluid with a free surface in a circular cylindrical container accelerating parallel to its axis is considered. A numerical procedure is developed and some interesting motions exhibiting the development of breakers, splashing and sustained oscillations of the surface are obtained by machine computation.

1. Introduction

The problem of fluid motion in a cylindrical container of circular cross-section due to a time-varying acceleration of the cylinder in the axial direction arises in connexion with the study of the dynamics of a liquid propellant in a rocket. This was the primary motivation for this study; however, the results which describe large amplitude motions of the surface of the fluid are of interest in themselves.

Concus (1962, 1964) considered finite amplitude motion in the two-dimensional case. Satterlee & Reynolds (1964) give an extensive bibliography of related work in this field and discuss the assumptions which are made in this paper; in particular, the dependence of the stability of the symmetric mode on the Bond number and contact angle is shown in their figure 6. The method developed in this paper is valid in both the stable and unstable regions and examples of both types of motion are computed.

A numerical procedure is designed for the simulation on a computer of the behaviour of the surface of the fluid. The method of solving the Eulerian equations is based on a Fourier series representation for the velocity potential with time dependent coefficients which are numerically determined from the free surface boundary conditions. Simultaneously, the motion of the free surface is determined using the method of characteristics which amounts to following the motion of individual fluid particles on the surface. Several interesting types of surface behaviour are obtained for various initial surface shapes depending on the acceleration and the surface tension. These results are exhibited graphically in the figures at the end of the paper. A detailed comparison with experimental results has not been made; however, recent unpublished work of Satterlee (private communication) shows at least qualitative agreement with the results of this paper.

2. Formulation of the equations of motion

Let $\mathbf{v}(r, z, t)$ be the axially symmetric velocity of a point (r, θ, z) in the fluid at time t . It is assumed that the flow is irrotational, i.e. that $\nabla \times \mathbf{v} = 0$, so that

there exists a velocity potential $\phi(r, z, t)$ such that $\mathbf{v} = \nabla\phi$. The geometry is indicated in figure 1.

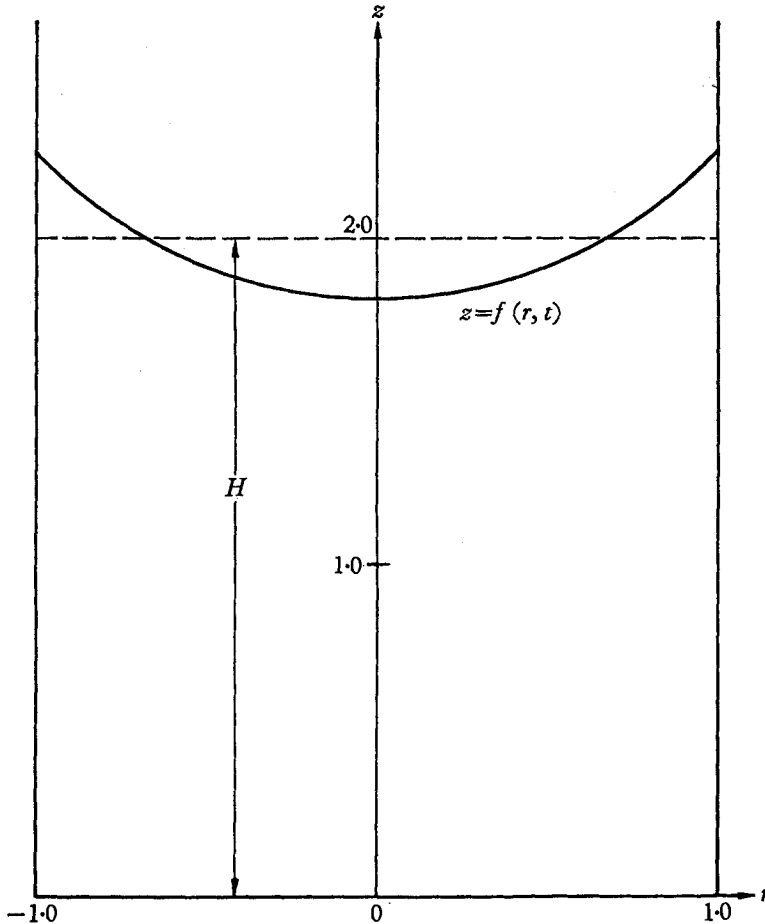


FIGURE 1. Co-ordinate system and hemispherical initial shape with $H = 2.0$ and $r_0 = 1.0$.

Since the flow is assumed incompressible, the equation of continuity implies that $\nabla \cdot \mathbf{v} = 0$ and hence that the velocity potential satisfies Laplace's equation in the interior of the fluid; i.e.

$$\phi_{rr} + (1/r)\phi_r + \phi_{zz} = 0 \quad (1)$$

for $t \geq 0$, $0 < r < r_0$, $0 \leq \theta < 2\pi$, $0 < z < f(r, t)$ where $z = f(r, t)$ is the equation of the free surface. The normal derivative is assumed to be zero on the fixed boundaries, i.e.

$$\left. \begin{aligned} \phi_r(0, z, t) &= 0 & \text{for } 0 \leq z \leq f(0, t) & (t \geq 0), \\ \phi_r(r_0, z, t) &= 0 & \text{for } 0 \leq z \leq f(r_0, t) & (t \geq 0), \\ \phi_z(r, 0, t) &= 0 & \text{for } 0 \leq r \leq r_0 & (t \geq 0). \end{aligned} \right\} \quad (2)$$

The free surface boundary condition follows from Euler's equation for inviscid flow

$$\mathbf{v}_t + (\mathbf{v} \cdot \nabla) \mathbf{v} = -(\nabla P/\rho) + \mathbf{g}$$

(Landau & Lifshitz 1959, p. 3), where $P(r, z, t)$ is the pressure at the point (r, θ) at time t and ρ is the density constant for the incompressible flow. This equation is identically satisfied in the interior if $\nabla \times \mathbf{v} = 0$ (Landau & Lifshitz 1959, p. 21). With the acceleration $\mathbf{g}(z, t)$ written as the gradient of a potential $U(z, t) = \alpha(t)g_0z$ where g_0 has the dimensions of acceleration, Euler's equation has as a first integral Bernoulli's equation

$$\phi_t + \frac{v^2}{2} + \frac{P}{\rho} - U = C(t). \quad (3)$$

If, for the present, surface tension is neglected, the fluid pressure $P(r, z, t)$ at the surface $z = f(r, t)$ is equal to a constant P_0 , the gas pressure at the fluid gas interface. Bernoulli's equation can then be written in the form of a boundary condition

$$\phi_t = \alpha(t)(z - H) - \frac{1}{2}(\phi_r^2 + \phi_t^2) \quad (4)$$

on the free surface $z = f(r, t)$ for $0 < r < 1$ and $t \geq 0$. In this equation H is some average height and for convenience we choose $C(t) = P_0/\rho - \alpha(t)Hg_0$. The coordinates have been normalized by dividing distances by r_0 , time by $(r_0/g_0)^{\frac{1}{2}}$ and the velocity potential by $(r_0^3g_0)^{\frac{1}{2}}$. Laplace's equation and the boundary conditions (2) remain invariant under this normalization.

The remaining equation, which together with (4) relates the motion of the surface to the potential, follows from $\mathbf{v} = (v_1, v_2) = d\mathbf{r}/dt$ where $\mathbf{r}(t)$ is a point in the fluid corresponding to (r, z) and t has been introduced as a parameter. This equation for points on the surface $z = f(r, t)$ can be written in component form with

$$\mathbf{r}(t)|_{z=f(r,t)} = \{r(t), f(r(t), t)\}$$

as

$$dr/dt = v_1 = \phi_r, \quad df/dt = v_2 = \phi_z. \quad (5)$$

Using the fact that the total derivative

$$df/dt = f_t + f_r(dr/dt),$$

these equations (5) can be combined into the single first-order partial differential equation

$$f_t = \phi_z - \phi_r f_r \quad (5')$$

on $z = f(r, t)$ for $0 < r < 1$ and $t \geq 0$. The curves $r = r(t)$ and $z = f(r(t), t)$ satisfying (5) are then the characteristic curves of the partial differential equation (5') (Courant & Hilbert 1962, p. 62).

The following initial conditions are imposed:

$$\left. \begin{aligned} f(r, 0) &= f_0(r) & \text{for } 0 \leq r \leq 1, \\ \phi(r, z, 0) &= 0 & \text{for } 0 \leq r \leq 1, \quad 0 \leq z \leq f_0(r), \\ \text{and} \quad \alpha(0) &= 0. \end{aligned} \right\} \quad (6)$$

Laplace's equation (1), together with the boundary conditions (2), (4), and (5) or (5') and the initial conditions (6) define the free surface boundary-value problem to be solved.

If surface tension is taken into account, the fluid pressure $P(r, \theta, z, t)$ at the surface is no longer equal to the constant P_0 but instead satisfies the relation

$$P = P_0 - \sigma \left(\frac{1}{R_1} + \frac{1}{R_2} \right),$$

where σ is the surface tension and R_1 and R_2 are the principal radii of curvature of the surface (Landau & Lifshitz 1959, p. 231). The radii of curvature are related to r and $f(r, t)$ by the equations

$$\frac{1}{R_1} = \frac{f_{rr}}{(1+f_r^2)^{\frac{3}{2}}}, \quad \frac{1}{R_2} = \frac{f_r}{r(1+f_r^2)^{\frac{3}{2}}}.$$

Including the surface tension term in Bernoulli's equation (3) leads to the following equation

$$\phi_t = \alpha(t) g_0 z - \frac{v^2}{2} - \frac{P_0}{\rho} + C(t) + \frac{\sigma}{\rho} \left[\frac{f_r}{r(1+f_r^2)^{\frac{3}{2}}} + \frac{f_{rr}}{(1+f_r^2)^{\frac{3}{2}}} \right]$$

on the free surface $z = f(r, t)$ ($0 < r < 1, t \geq 0$). A convenient normalization when surface tension is being taken into account is to divide distances by r_0 , time by $[\rho r_0^3 / \sigma(1+B)]^{\frac{1}{2}}$ and the velocity potential by $[(1+B)\sigma r_0 / \rho]^{\frac{1}{2}}$ where $B = \rho r_0^2 g_0 / \sigma$ is a dimensionless number. The above equation then becomes

$$\phi_t = \frac{\alpha(t)}{1+1/B} (z-H) - \frac{1}{2} [\phi_r^2 + \phi_z^2] + \frac{1}{1+B} \left[\frac{f_r}{r(1+f_r^2)^{\frac{3}{2}}} + \frac{f_{rr}}{(1+f_r^2)^{\frac{3}{2}}} \right] \quad (7)$$

on the surface $z = f(r, t)$ and as before $C(t) = (P_0/\rho) - \alpha(t) H g_0$ has been chosen for convenience. Laplace's equation and the boundary conditions (2) remain invariant under this normalization. This equation then replaces the free-surface boundary condition (4) when surface tension is taken into account.

The surface tension term in equation (7) is included in the computation as a smoothing term, its value being computed from the previous behaviour of the surface shape as described in the next section.

3. Method of solution

The approach taken in this paper is to develop a series representation for the velocity potential satisfying Laplace's equation in the interior and the boundary conditions (2) and to determine the time-dependent coefficients numerically by imposing the free surface-boundary conditions (4) and (5).

The representation for the velocity potential is determined by a separation of variables approach. It is assumed that

$$\phi(r, z, t) = C(t) R(r) Z(z).$$

This leads to the following ordinary differential equations and boundary conditions for $R(r)$ and $Z(z)$:

$$R'' + (1/r)R' + \kappa R = 0, \quad R'(0) = R'(1) = 0$$

and

$$Z'' - \kappa Z = 0, \quad Z'(0) = 0.$$

This set of equations has a non-zero solution for a countable number of values of

the constant κ ; since Laplace's equation is a linear differential equation, a linear combination of these solutions is a formal solution, i.e. the velocity potential is given by

$$\phi(r, z, t) = \sum_{n=0}^{\infty} C_n(t) J_0(\lambda_n r) \left[\frac{\cosh(\lambda_n z)}{\cosh(\lambda_n H)} \right] \tag{8}$$

and the velocity components are given by

$$\left. \begin{aligned} \phi_r(r, z, t) &= - \sum_{n=0}^{\infty} \lambda_n C_n(t) J_1(\lambda_n r) \left[\frac{\cosh(\lambda_n z)}{\cosh(\lambda_n H)} \right], \\ \phi_z(r, z, t) &= \sum_{n=0}^{\infty} \lambda_n C_n(t) J_0(\lambda_n r) \left[\frac{\sinh(\lambda_n z)}{\cosh(\lambda_n H)} \right], \end{aligned} \right\} \tag{9}$$

where $J_0(\lambda_n r)$ and $J_1(\lambda_n r)$ are the zeroth and first-order Bessel functions respectively and λ_n ($n = 0, 1, 2, \dots$), are the roots of $J_1(\lambda_n) = 0$; i.e. $\lambda_0 = 0, \lambda_1 = 3.8317\dots$, etc. A direct proof of convergence of this series is not made; rather, the plausibility of convergence of an elliptic partial differential equation on a square (to which the present problem can be transformed) is presented in the Appendix.

A numerical procedure for approximating the coefficients using the free surface-boundary conditions is now described. First, let

$$F_n(r, t) = J_0(\lambda_n r) \frac{\cosh[\lambda_n f(r, t)]}{\cosh(\lambda_n H)} \quad (n = 0, 1, 2, \dots) \tag{10}$$

and
$$B(r, t) = \alpha(t) [f(r, t) - H] - \frac{1}{2} [\phi_r^2(r, f(r, t), t) + \phi_z^2(r, f(r, t), t)].$$

Bernoulli's equation, (4), can then be written in the form

$$\sum_{n=0}^{\infty} C'_n(t) F_n(r, t) = B(r, t). \tag{11}$$

The set of functions $F_n(r, t)$ ($n = 0, 1, 2, \dots$), is orthonormalized with the weight function $w(r) = r$ on $[0, 1]$ for each $t \geq 0$ to obtain the orthonormal set $G_n(r, t)$ ($n = 0, 1, 2, \dots$). The orthonormal set can be written in terms of the original functions

$$G_n(r, t) = \sum_{m=0}^n a_{nm}(t) F_m(r, t) \quad (n = 0, 1, 2, \dots), \tag{12}$$

and conversely the original functions can be written in terms of the orthonormalized functions

$$F_n(r, t) = \sum_{m=0}^{\infty} b_{nm}(t) G_m(r, t) \quad (n = 0, 1, 2, \dots), \tag{12'}$$

where for each $n \geq 0$, the $a_{nm}(t)$ and the $b_{nm}(t)$ ($m = 0, 1, 2, \dots, n$), can be written in terms of the time-dependent inner products

$$(F_i, F_j) = \int_0^1 r F_i(r, t) F_j(r, t) dr \quad (i = 0, \dots, n; j = i, \dots, n), \tag{13}$$

as is exhibited in the following sequence of equations (cf. Walsh 1956, p. 113 for the time-independent case):

$$\begin{aligned}
 G_0(r, t) &= F_0(r, t) = 1, \\
 G_1(r, t) &= F_1(r, t)/(F_1, F_1)^{\frac{1}{2}}, \\
 G_2(r, t) &= F_2(r, t) - (F_2, G_1) G_1(r, t)/[(F_2, F_2) - (F_2, G_1)^2]^{\frac{1}{2}}, \\
 &\dots\dots\dots \\
 G_n(r, t) &= \frac{F_n(r, t) - (F_n, G_{n-1}) G_{n-1}(r, t) - \dots - (F_n, G_1) G_1(r, t)}{[(F_n, F_n) - (F_n, G_{n-1})^2 - \dots - (F_n, G_1)^2]^{\frac{1}{2}}}.
 \end{aligned}$$

Bernoulli's equation can then be written in the equivalent form

$$\sum_{n=0}^{\infty} \gamma(t) G_n(r, t) = B(r, t),$$

where (14)

$$\gamma_n(t) = \sum_{m=n}^{\infty} C'_m(t) b_{nm}(t).$$

By virtue of the orthonormality of the functions $G_n(r, t)$, it follows that

$$\gamma_n(t) = \int_0^1 r G_n(r, t) B(r, t) dr \quad (n = 0, 1, 2, \dots). \tag{15}$$

The series (8) for the velocity potential is now truncated after N terms and the first N coefficients are determined by a numerical algorithm which involves evaluating the definite integrals (13) and (15) and solving a system of first-order ordinary differential equations at each time step. Truncating the series (14) after N terms, the coefficients $C'_n(t)$ ($n = 0, \dots, N - 1$) can be written in terms of the $\gamma_n(t)$ and the $b_{nm}(t)$ ($n = 0, \dots, N - 1; m = n, \dots, N - 1$) which in turn are given in terms of the $\frac{1}{2}N^2 + N$ definite integrals appearing in equations (13) and (15), whose integrands depend upon $C_n(t)$ ($n = 0, \dots, N - 1$), $r(t)$ and $f(r(t), t)$ (using equations (8), (10), (12), and (15)). In other words

$$C'_n(t) = \mathcal{F}_n(C_k, f, r) \quad (n = 0, \dots, N - 1),$$

where for each $n, k = 0, \dots, N - 1$. These equations together with (5) for a finite number of points $(r_m(t), f_m(t))$ ($m = 1, \dots, M$) on the free surface can be written as a first-order autonomous system

$$\dot{x} = \mathcal{F}(x), \tag{16}$$

where $x(t) = (C_n(t), r_m(t), f_m(t))$ and $\mathcal{F}(x) = (\mathcal{F}_n(x), \phi_r^{(m)}(x), \phi_z^{(m)}(x))$ ($n = 0, \dots, N - 1$) and ($m = 1, \dots, M$), and where $f_m(t) = f(r_m(t), t)$. The functions $\phi_r^{(m)}$ and $\phi_z^{(m)}$ ($m = 1, \dots, M$), are defined in terms of x by the series (9); i.e.

$$\phi_r^{(m)}(x) = - \sum_{n=0}^{N-1} \lambda_n C_n(t) J_1(\lambda_n r_m) \left[\frac{\cosh(\lambda_n f_m)}{\cosh(\lambda_n H)} \right],$$

and
$$\phi_z^{(m)}(x) = \sum_{n=0}^{N-1} \lambda_n C_n(t) J_0(\lambda_n r_m) \left[\frac{\sinh(\lambda_n f_m)}{\cosh(\lambda_n H)} \right] \quad (m = 1, \dots, M).$$

The initial conditions used in the solution of (16) are determined by the assumption that the fluid is initially at rest and by a knowledge of the initial

shape of the free surface; i.e. we set $C_n(0) = 0$ ($n = 0, \dots, N-1$), and choose some distribution of points on the given initial surface, $(r_m(0), f_m(0))$ ($m = 1, \dots, M$). The $\frac{1}{2}N^2 + N$ definite integrals, (13) and (15) are then evaluated and the p th order system of first-order ordinary differential equations (16), where $p = M + N$, is solved by a predictor-corrector method, the 'modified Euler' method, to move ahead an increment of time. The time-dependent coefficients and the motion of individual particles on the free surface are determined in this way.

This method has the advantage of not requiring the function describing the surface shape $f(r, t)$ to be single valued. The choice of the numbers M and N and of the initial distribution of points on the surface will be discussed in the next section.

If surface tension is taken into account as a smoothing term, the first and second partial derivatives of $f(r, t)$ with respect to r must be evaluated and included in the Bernoulli equation as in equation (7). This was originally done by a differencing scheme. This however was not accurate enough to give meaningful results. The surface tension term

$$Tf = \frac{1}{r} \frac{\partial}{\partial r} \left[\frac{rf_r}{(1+f_r^2)^{\frac{1}{2}}} \right]$$

was then considered as an operator on some function space and the first variation in T corresponding to a small variation in $f(r, t)$, $\delta f(r, t) = f(r, t + \Delta t) - f(r, t)$, resulting from a time increment Δt was found; i.e.

$$T(f + \delta f) = Tf + \frac{1}{r} \frac{\partial}{\partial r} \left[\frac{r(\delta f)_r}{(1+f_r^2)^{\frac{1}{2}}} \right] + O(\delta f)_r^2,$$

where $(\delta f)_r = \phi_{rr} \Delta t + O(\Delta t^2)$, since from (5), $\delta f = \phi_z \Delta t + O(\Delta t^2)$. The ratio of the remainder to the first-order correction is proportional to Δt and this approximation can therefore be made sufficiently accurate by making Δt small enough. This is the method used in computing the surface tension term in the numerical programme.

For hemispherical initial shapes of radius R

$$f_0(r) = R - (R^2 - r^2)^{\frac{1}{2}}. \quad (17)$$

This function satisfies the ordinary differential equation

$$\frac{1}{r} \frac{\partial}{\partial r} \left[\frac{rf'_0(r)}{(1+f'_0(r)^2)^{\frac{1}{2}}} \right] = \frac{2}{R}$$

and it is convenient to subtract the constant $2/R$ from the Bernoulli equation (7) and add it to the function $C(t)$ so that Tf is initially zero.

4. Numerical results

The numerical results are for two basic cases:

(1) $\alpha(t) = 1.0$ for $t > 0$, i.e. the cylinder is being accelerated in such a manner that the fluid runs to the opposite end of the container (figures 2-6). This is characterized by the case of an upside-down cylindrical container at the earth's surface, gravity acting to pull the liquid out of the container.

(2) $\alpha(t) = -1.0$ for $t > 0$, i.e. the cylinder is being accelerated in such a manner that the fluid remains in the bottom of the cylinder (figures 7–9). This is characterized by the case of an upright cylindrical container of liquid at the earth's surface, gravity acting to keep the liquid in the container.

These cases were considered for different initial surface shapes and for varying degrees of surface tension from $\beta \equiv B^{-1} = 0$ (no surface tension) to $\beta = 0.05$, a typical example of which is water in a 0.8 in. diameter cylinder. In the latter case there is a significant amount of surface tension although the acceleration force is still dominant. The majority of the cases were run with a hemispherical initial shape, defined by equation (17), for different values of the radius $R = \sec \theta_0$, where θ_0 is the initial contact angle that the surface makes with the wall. A summary of the cases studied is given in table 1, where t is given in seconds for r_0 given in feet.

| Figure no. | $\alpha(t)$ | β | Initial shape | H | θ_0 | $\Delta t/r_0^{\frac{1}{2}}$ | $t_{\text{final}}/r_0^{\frac{1}{2}}$ |
|------------|-------------|---------|--------------------|-----|------------|------------------------------|--------------------------------------|
| 2 | +1.0 | 0 | Hemispherical | 2.0 | 45° | 0.0177 | 0.195 |
| — | +1.0 | 0 | Hemispherical | 2.0 | 22.5° | 0.0177 | 0.14 |
| — | +1.0 | 0 | Hemispherical | 0.4 | 45° | 0.0266 | 0.16 |
| 5 | +1.0 | 0.005 | Hemispherical | 2.0 | 45° | 0.0177 | 0.16 |
| 6 | +1.0 | 0.05 | Flat with meniscus | 2.0 | 0° | 0.0350 | 0.49 |
| 7 | -1.0 | 0 | Hemispherical | 2.0 | 45° | 0.0266 | 0.40 |
| 8 | -1.0 | 0.05 | Hemispherical | 2.0 | 45° | 0.0266 | 0.48 |
| 9 | -1.0 | 0.05 | Hemispherical | 2.0 | 15° | 0.0266 | 0.48 |

TABLE 1. Summary of the cases studied

The values of M and N that were used were determined by experiment. It was found that good results were obtained with the number of points in the r -mesh $M = 45$, the distribution being denser near the wall, i.e. near $r = 1$. After making runs with $N = 5, 6, 10, 11, 15$, and 16 terms in the series, it appeared that ten terms in the series would be sufficient to obtain reasonably accurate results. This is exhibited in figure 4 where the coefficients for one of the runs, starting with a hemispherical initial shape and using ten terms, are plotted as a function of time, and by the fact that carrying more terms than ten did not affect the value of the first ten terms significantly. The variation in the volume of the liquid is a measure of the accuracy of computation. It was found that with the choice of M and N indicated above, the volume varies by less than 0.01 % per iteration for the largest time step that was used.

In the course of the study, large amplitude motions were calculated and some interesting phenomena occurred. For example, in figure 2, for the case with gravity acting to pull the fluid out of the container and no surface tension effect present, breakers similar to those in Stoker (1957, p. 367) developed at the wall of the container. Figures 2 and 5–9 are reproductions of piecewise linear plots made by the SC 4020 plotter directly from the computer results, and the breakers in figure 2 therefore look somewhat jagged. Figure 3 shows the development of the breakers

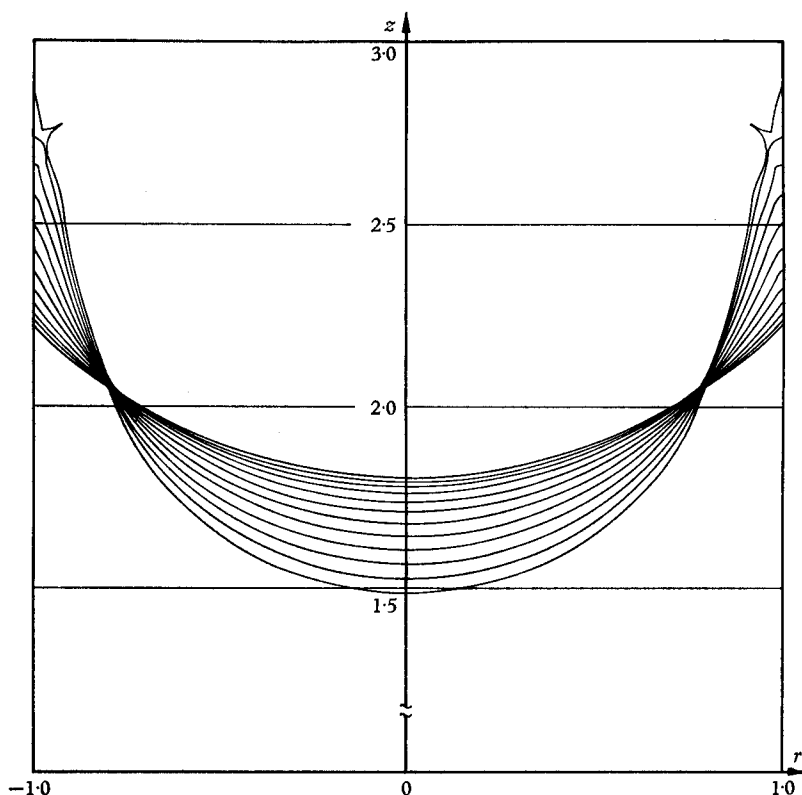


FIGURE 2. Hemispherical initial shape with $H = 2.0$, $\alpha(t) = +1$,
 $\beta = 0$, $\theta_0 = 45^\circ$ and $\Delta t = 0.0177 r_0^{\frac{1}{2}}$ sec.

in detail for the case in figure 2 with a smaller time step. The coefficients $C_n(t)$ ($n = 0, \dots, 9$), for this case are plotted in figure 4 as a function of time. The velocity potential and velocity components at any point in the fluid for

$$0 \leq t \leq t_{\text{final}}$$

for this case can be computed from equations (8) and (9) using these values for the coefficients. It was observed that varying the time step for this case had little or no effect on the overall behaviour and the breakers appeared at almost exactly the same time when different time steps were used. As an indication of the 7094 computer time required, the total time of computation for the fluid motion shown in figure 2 was 6 minutes. However, not every surface shape that was computed could be shown in the figures presented here and still retain clarity. In figure 2, for example, every fifth shape that was computed is shown in the figure.

The time at which the breakers occurred was found to be very sensitive to small changes in the initial shape, i.e. to small amplitude variations in the initial shape. For example, a deviation from the hemispherical shape of figure 2 by 2% at two or three points on the surface caused a 20% decrease in the time at which the breakers occurred. The qualitative behaviour was much the same for

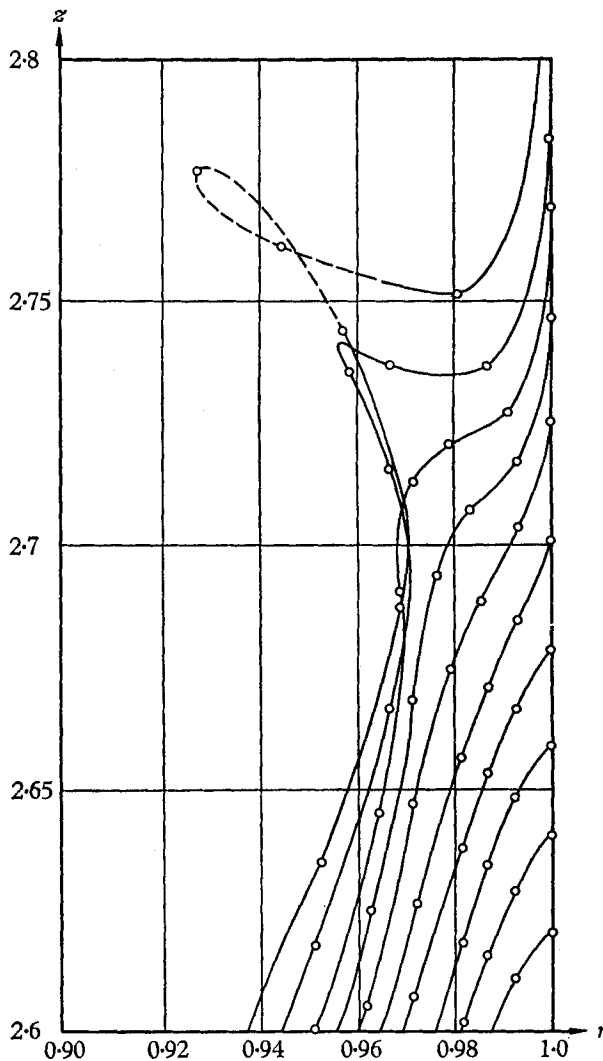


FIGURE 3. The breakers at the wall for the case in figure 2.

smaller contact angles, θ_0 , the time at which the breakers occurred being proportionately smaller (table 1). The qualitative behaviour was also very much the same for different volumes of fluid although a bottom effect was observed in the case of small volumes. The time at which the breakers occurred did not differ much for different volumes.

Surface tension had a smoothing effect which eliminated the breakers for sufficiently large β ; however, in the computation the surface tension had the effect of over-correcting any unduly large curvature in the surface such as that which develops when breakers start to form. This results in undamped oscillations in this term. This was eliminated by going to a variable time step in order to maintain the growth of the surface tension term smaller than some prescribed bound. This led to a reduction in the time step to so small a value as to make it impractical

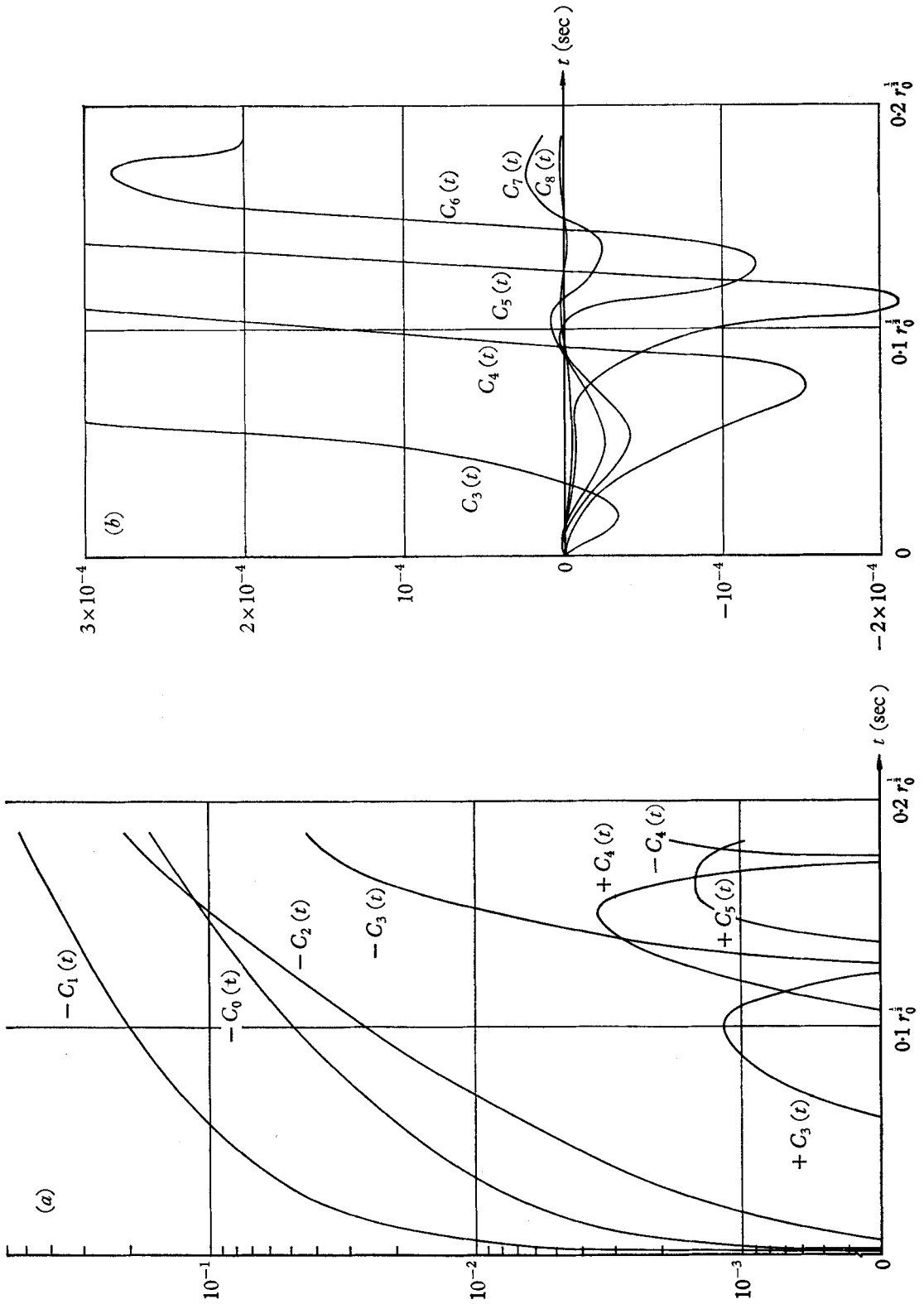


FIGURE 4. The time variation of the coefficients for the case in figure 2.

to continue the computation. Nevertheless, some interesting results were obtained before this occurred (see for example figure 5, which corresponds to the case shown in figure 2 with a small surface tension effect included). The smoothing effect is particularly evident near the wall of the container.

The case of a nearly flat initial surface shape with a meniscus at the wall was next considered with $\alpha(t) = +1.0$ and $\beta = 0.05$. This resulted in a considerable

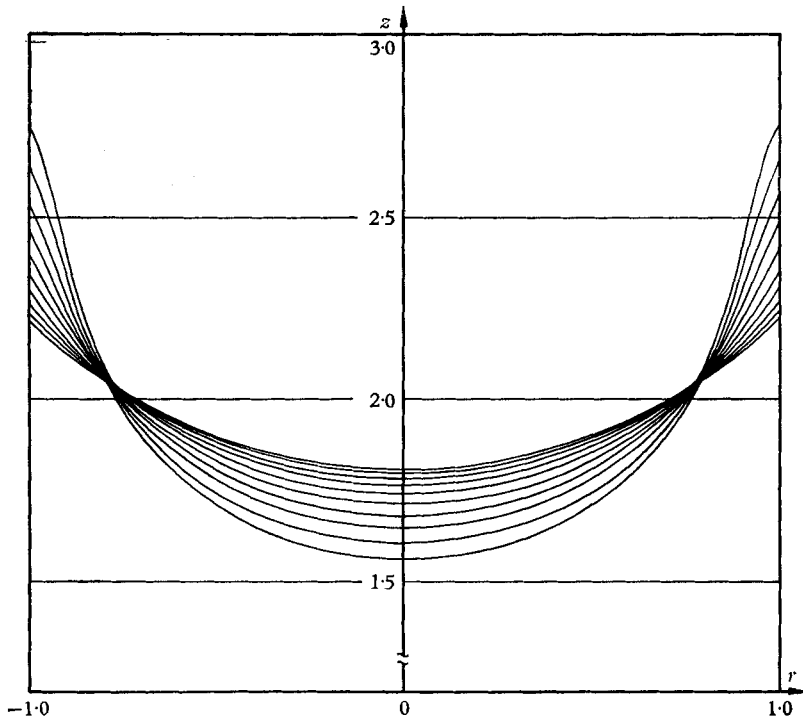


FIGURE 5. Hemispherical initial shape with $H = 2.0$, $\alpha(t) = +1$, $\beta = 0.005$, $\theta_0 = 45^\circ$ and $\Delta t = 0.0177 r_0^{\frac{1}{2}}$ sec.

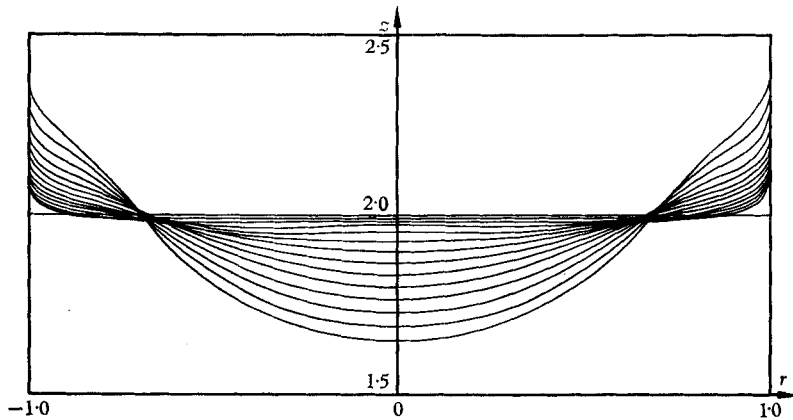


FIGURE 6. Flat initial shape with a meniscus at the wall, $H = 2.0$, $\alpha(t) = +1$, $\beta = 0.05$, $\theta_0 = 0^\circ$ and $\Delta t = 0.0350 r_0^{\frac{1}{2}}$ sec.

change in the surface shape before the time step was reduced to a prohibitively small value and indicates the ability of the programme to handle zero-degree contact angle (figure 6). Without surface tension the initially flat surface moved very little before breakers developed at the wall.

The case of the acceleration growing linearly with time, $\alpha(t) = kt$, was also considered with a hemispherical initial shape and no surface tension effect, $\beta = 0$. The results were qualitatively the same as those depicted in figure 2; the time at which the breakers occurred increased with decreasing k .

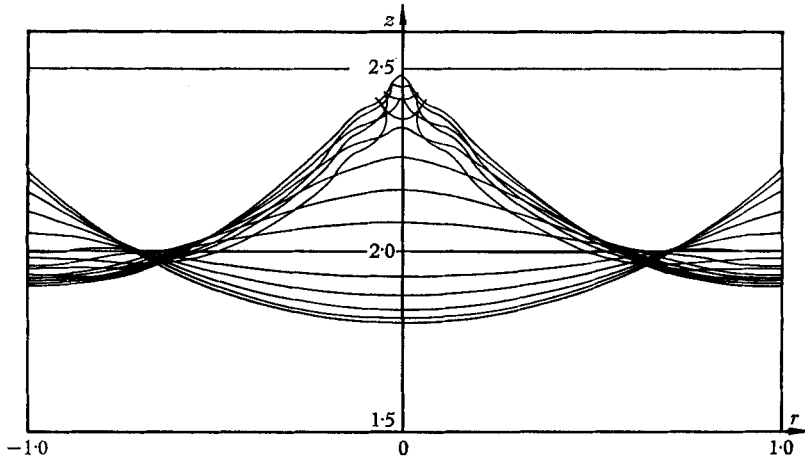


FIGURE 7. Hemispherical initial shape with $H = 2.0$, $\alpha(t) = -1$, $\beta = 0$, $\theta_0 = 45^\circ$ and $\Delta t = 0.0266 r_0^{1/2}$ sec.

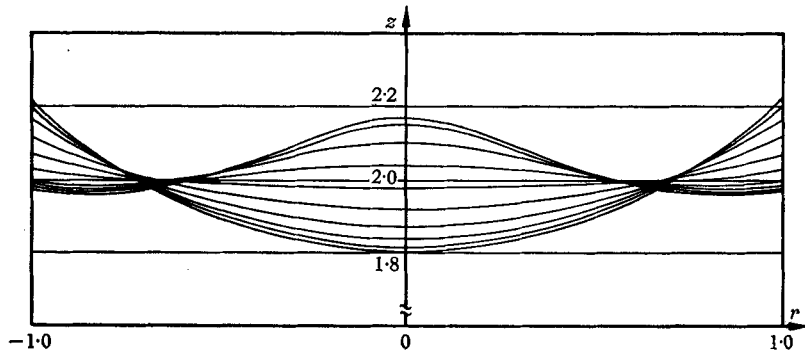


FIGURE 8. Hemispherical initial shape with $H = 2.0$, $\alpha(t) = -1$, $\beta = 0.05$, $\theta_0 = 45^\circ$ and $\Delta t = 0.0266 r_0^{1/2}$ sec.

The case of gravity acting to keep the fluid in the container, $\alpha(t) = -1$, was next considered for a hemispherical initial shape. Some very interesting kinds of oscillations were obtained. The relative size of the surface tension, gravity and the initial contact angle determined whether or not a splash developed on the surface. In figure 7, for example, with no surface tension, $\beta = 0$, and an initial contact angle of 45° , a crown-shaped splash developed at the centre of the fluid.

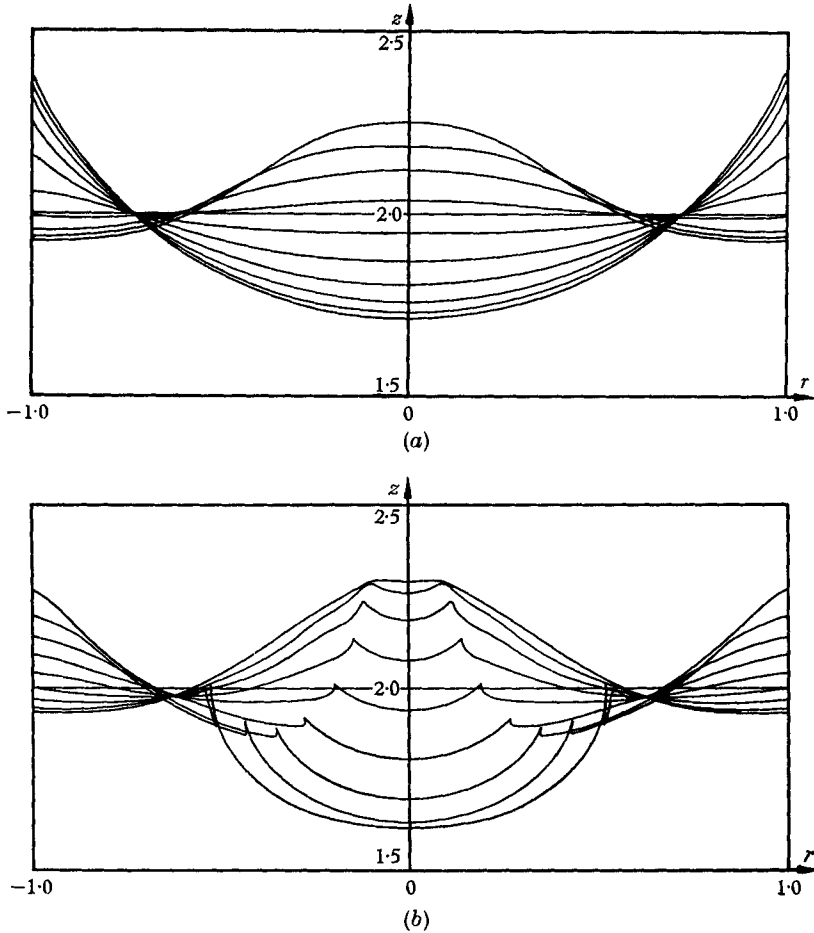


FIGURE 9. (a) Hemispherical initial shape with $H = 2.0$, $\alpha(t) = -1$, $\beta = 0.05$, $\theta_0 = 15^\circ$ and $\Delta t = 0.0266 r_0^{\frac{1}{2}}$ sec. (b) A continuation of figure 9 (a).

It was found that with the initial contact angle equal to 45° and a small surface tension effect, $\beta = 0.005$, an example of which is given by water in a 2.5 in. cylinder, the surface goes through one and a half oscillations before a splash starts to develop. With the initial contact angle again equal to 45° and a larger surface tension effect, $\beta = 0.05$, e.g. water in a 0.8 in. diameter cylinder, no splash develops and several complete oscillations of the surface were computed. Half of the first complete oscillation is shown in figure 8. It is interesting to note that the average period of oscillation, $T = 0.485 r_0^{\frac{1}{2}}$ sec (r_0 in ft.), is somewhat larger than that given by the linear theory, $T = 0.434 r_0^{\frac{1}{2}}$ sec \dagger .

In the final case with $\alpha(t) = -1.0$, $\beta = 0.05$ and $\theta_0 = 15^\circ$ a splash again develops due to the larger amount of potential energy in the initial surface shape even though the amount of surface tension is the same as in the previous case (figures 9 (a) and (b)).

\dagger Communicated by P. Concus.

This work was carried out under the Lockheed Independent Research and Development Programmes. The authors wish to thank W. E. Jahsman, P. Concus, and R. J. Dickson for their many enlightening discussions without which this work would not have been possible and R. L. Causey for suggesting the orthonormalization.

REFERENCES

CONCUS, P. 1962 Standing capillary-gravity waves of finite amplitude. *J. Fluid Mech.* **14**, 568-76.
 CONCUS, P. 1964 Standing capillary-gravity waves of finite amplitude: corrigendum. *J. Fluid Mech.* **19**, 264-66.
 COURANT, R. & HILBERT, D. 1962 *Methods of Mathematical Physics*, Vol. II. New York: Interscience.
 ITO, S. 1957 Fundamental solutions of parabolic differential equations and boundary value problems. *Jap. J. Math.* **27**, 55.
 LANDAU, L. D. & LIFSHITZ, E. M. 1959 *Fluid Mechanics*. London: Pergamon Press.
 SATTERLEE, H. M. & REYNOLDS, W. C. 1964 The dynamics of the free liquid surface in cylindrical containers under strong capillary and weak gravity conditions. Stanford University Department of Mech. Eng., Thermo. Sci. Div. T.R. no. LG-2.
 STOKER, J. J. 1957 *Water Waves*. New York: Interscience.
 WALSH, J. L. 1956 *Interpolation and Approximation*. Rhode Is.: American Math. Soc. Publication.

Appendix

Many authors have considered the problem of eigenfunction expansions for formally self-adjoint elliptic operators of the type

$$A\psi(x, t) = (a(x, t))^{-\frac{1}{2}} \frac{\partial}{\partial x^i} \left[a^{ij}(x, t) (a(x, t))^{\frac{1}{2}} \frac{\partial \psi}{\partial x^j} \right] + c(x, t) \psi(x, t)$$

in time independent regions where

$$a(x, t) = \det [a_{ij}(x, t)] = \det [a^{ij}(x, t)]^{-1},$$

and the coefficients are assumed to have certain smoothness properties. Typical boundary conditions have the form

$$\alpha(x, t) \psi(x, t) + \beta(x, t) \frac{\partial \psi(x, t)}{\partial n} = G(x, t).$$

(See, for example, Ito 1957, pp. 55-102, where sufficient conditions for such expansions have been given.)

The operator A is the type that is obtained in the problem being considered here under the transformation of co-ordinates $\rho = z/f(r, t)$ which takes a time dependent domain of the type shown in figure 1 into a square. In fact, for a general admissible transformation of co-ordinates with the Reimann metric given by $ds^2 = a_{ij}(x, t) dx^i dx^j$, the Laplacian has the form given above with $c(x, t) \equiv 0$. For the transformation in question with $x = (r, \rho, \theta)$

$$[a^{ij}(x, t)] = \begin{bmatrix} 1 & -\frac{f_r(r, t)\rho}{f(r, t)} & 0 \\ -\frac{f_r(r, t)\rho}{f(r, t)} & \frac{[1+f_r^2(r, t)\rho^2]}{f^2(r, t)} & 0 \\ 0 & 0 & \frac{1}{r^2} \end{bmatrix}$$

and $\det [a_{ij}(x, t)] = r^2 f^2(r, t)$. $[a_{ij}(x, t)]$ is therefore a positive definite matrix provided $rf(r, t) \neq 0$.

Let $\psi(r, \rho, t) = \phi(r, \rho f(r, t), t)$.

Then ψ must satisfy the elliptic partial differential equation

$$\frac{1}{|rf|} \left\{ \frac{\partial}{\partial r} \left[|rf| \left(\psi_r - \frac{f_r \rho}{f} \psi_\rho \right) \right] + \frac{\partial}{\partial \rho} \left[|rf| \left(-\frac{f_r \rho}{f} \psi_r + \frac{1 + f_r^2 \rho^2}{f^2} \psi_\rho \right) \right] \right\} = \theta$$

and boundary conditions which may be put into a form similar to the above:

$$\frac{\partial \psi}{\partial n} = 0 \begin{cases} \text{on } r = 0, 1 & \text{for } 0 \leq \rho \leq 1, \\ \text{and on } \rho = 0 & \text{for } 0 \leq r \leq 1, \end{cases}$$

and $\psi(r, 1, t) = G(r, t)$ for $0 \leq r \leq 1$, and $t \geq 0$, where

$$G(r, t) = -\frac{1}{2} \lim_{t' \rightarrow t^-} \int_0^{t'} \left\{ \psi_r^2(r, 1, \tau) - \frac{2f_r(r, \tau)}{f(r, \tau)} \psi_r(r, 1, \tau) \psi_\rho(r, 1, \tau) + \frac{[1 + f_r^2(r, \tau)]}{f^2(r, \tau)} \psi_\rho^2(r, 1, \tau) \right\} d\tau$$

and where it has been assumed for convenience that the average height $H = 1$.

The function $f(r, t)$ must satisfy the first order partial differential equation

$$f_t(r, t) = -f_r(r, t) \psi_r(r, 1, t) + \frac{[1 + f_r^2(r, t)]}{f(r, t)} \psi_\rho(r, 1, t)$$

for $0 \leq r \leq 1$ and $t \geq 0$. The continuity conditions required in Ito (1957) as well as the conditions such that the transformation be admissible are satisfied if $f(r, t)$ is a non-zero single-valued function of r and is sufficiently smooth for all $0 \leq r \leq 1$ and each $t \geq 0$. With the problem in this form, it seems plausible that, using the theorem on p. 89 of Ito (1957), the convergence of the series (8) can be established.